

## Current status of gravitational-wave observations

Stephen Fairhurst, Gianluca M Guidi,  
Patrice Hello, John T Whelan,  
Graham Woan

27 August 2009

**Abstract** The first generation of gravitational wave interferometric detectors has taken data at, or close to, their design sensitivity. This data has been searched for a broad range of gravitational wave signatures. An overview of gravitational wave search methods and results are presented. Searches for gravitational waves from unmodelled burst sources, compact binary coalescences, continuous wave sources and stochastic backgrounds are discussed.

---

Stephen Fairhurst  
Department of Physics and Astronomy  
Cardiff University, Cardiff, CF24 3AA, UK  
E-mail: [stephen.fairhurst@astro.cf.ac.uk](mailto:stephen.fairhurst@astro.cf.ac.uk)

Gianluca M Guidi  
Istituto di Fisica  
Via S Chiara 27, 61029, Urbino, IT  
Universita di Urbino, INFN Firenze  
E-mail: [gianluca.guidi@uniurb.it](mailto:gianluca.guidi@uniurb.it)

Patrice Hello  
LAL, Universite Paris-Sud, IN2P3/CNRS  
F-91898 Orsay, France  
E-mail: [hello@in2p3.lal.fr](mailto:hello@in2p3.lal.fr)

John T Whelan  
Center for Computational Relativity and Gravitation and School of Mathematical Sciences  
Rochester Institute of Technology, 85 Lomb Memorial Drive, Rochester, NY 14623, USA  
E-mail: [john.whelan@astro.rit.edu](mailto:john.whelan@astro.rit.edu)

Graham Woan  
Department of Physics & Astronomy  
University of Glasgow  
Glasgow G12 8QQ, UK  
E-mail: [graham@astro.gla.ac.uk](mailto:graham@astro.gla.ac.uk)

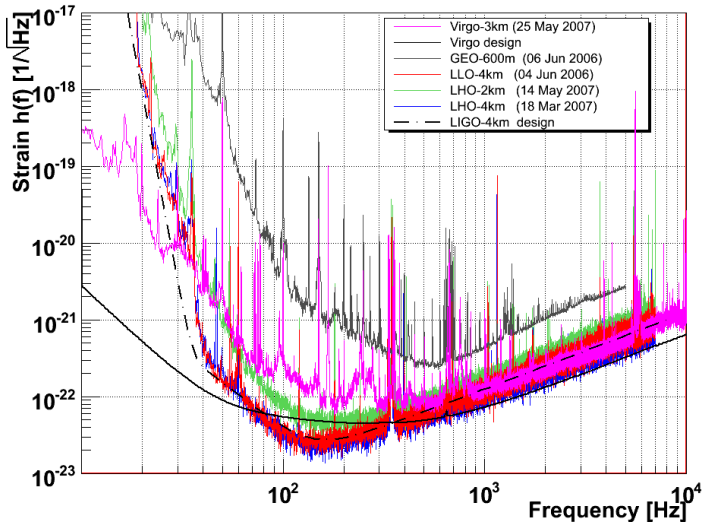


**Fig. 1** Typical spectral density of calibrated noise for the LIGO interferometers and GEO during the S5 run and for Virgo interferometer during the VSR1 run. Also displayed are the design sensitivities for the 4 km LIGO interferometers and for Virgo.

## 1 Introduction

The first generation of gravitational wave (GW) interferometric detectors has reached an unprecedented sensitivity to GW signals.

Six interferometric detectors completed commissioning activities and acquired scientific data over the last years. Three of them constitute the Laser Interferometric Gravitational-Wave Observatory (LIGO), a joint Caltech-MIT project supported by the National Science Foundation [1]. They are situated in the USA, one in Livingston, Louisiana (L1) and two, which share the same facilities, in Hanford, Washington (H1, H2). L1 and H1 are interferometers with arms of length 4 km, whereas H2 is a 2 km interferometer. Their first Science Run began in September 2002. Since then, four other science runs took place; between November 2005 and September 2007 they operated at their design sensitivity in a continuous data-taking mode in the 5th science run (S5).

The Virgo detector is a joint project of the CNRS and INFN, operated by the Virgo Collaboration at the European Gravitational Observatory - a CNRS-INFN joint venture with the mandate to build the interferometer [2]. Virgo is a 3 km interferometer near Pisa (Italy). Its first Science Run (VSR1) took place in May 2007–September 2007, with a sensitivity comparable to LIGO instruments above around 400 Hz and a better sensitivity below 30 Hz. (see Fig. 1).

---

Two additional interferometric detectors are part of the network of GW observatories: the Japanese TAMA project built a 300m interferometer near Tokyo, Japan [3] and the German-British GEO project built a 600m interferometer near Hannover, Germany [4]; early in its operation GEO joined with the LIGO Scientific Collaboration. The current sensitivity of TAMA and GEO is not comparable to LIGO and Virgo, and the latest scientific observational results are based on the analysis of S5/VSR1 data.

The LIGO S5 run collected a full year of triple detector coincidence interferometer data, whereas Virgo ran in science mode for about 110 days during VSR1. One of the most promising candidates for a GW detection is thought to be the signal originated during the coalescence of two neutron stars. The distance at which a system of two neutron stars of 1.4 solar masses can be detected by a gravitational wave observatory, with a signal to noise ratio of 8, has thus become a standard measure of the detectors' sensitivity. During the S5/VSR1 run, H1 reached a maximum sight distance of 35 Mpc, corresponding to a spherical observable volume of radius of 15 Mpc.

LIGO and Virgo signed an agreement to jointly analyze data from the four LIGO-Virgo interferometers collected after May 2007. The Data Analysis activity is run by four LIGO-Virgo search physics groups with different scientific targets: Burst, Compact Binary Coalescences, Continuous Waves and Stochastic Background, each aiming at the detection and characterisation of different sources of GWs. Even if this division is somehow arbitrary, it has become the accepted standard in GW data analysis.

Currently, a new joint run, S6/VSR2, is on-going. The goal is to improve the sensitivity of the detectors, Enhanced LIGO and Virgo+, by about a factor 2 over the course of the run, resulting in an observable volume of the universe of about an order of magnitude larger.

In the next sections of this article a general introduction to the methods applied and observational results obtained for the different targets will be presented.

## 2 Bursts

### 2.1 Introduction

Gravitational wave bursts are taken to be short signals, duration  $< 1$ s, with a large variety of possible waveforms, either wide or rather narrow-band in the frequency domain. GW bursts historically correspond to poorly modelled signals, due to the complex physics involved in the description of the sources, such as core collapse supernovae or mergers of two compact stars (black holes and/or neutron stars). Hence analysis methods seeking GW bursts must in general stay robust with respect to the expected waveforms. Moreover the benefit of running robust analysis methods is to stay wide open to the unexpected, something which is fine when in a discovery mode. This constraint can be relaxed somewhat if some additional information about the source is avail-

able from other astrophysical observations. Also, spectacular recent progress in numerical relativity has allowed for accurate modelling of GW sources. For the most important burst sources we have now at least an idea of what the emitted waveform looks like.

## 2.2 Sources of GW bursts

Core collapse supernova — the collapse of a massive star and neutron star formation — has long been envisaged as one of the first GW sources. Modern models now include 3D full relativistic hydrodynamical simulations together with detailed micro-physics [5, 6, 7, 8]. They predict the emission of GW signal during the fast gravitational collapse and bounce with a duration  $\sim 1$  ms and peak amplitude  $h \simeq 10^{-21}$  for sources located at 10 kpc. A longer (hundreds of ms) and in some cases stronger signal is also expected after the bounce due to hydrodynamical instabilities around the proto-neutron star.

Another source of GW bursts is the merger of two compact stars (black hole and/or neutron star) which generally results in a black hole, surrounded by a torus of matter if at least one of the progenitors is a neutron star. Progress in numerical relativity in recent years allows a clear picture of the merger of two black holes and a good prediction for the waveform [9, 10]. Good progress has been made too in modelling the merger of two neutron stars [11], which is an even more complex problem due to, for example, the role of the neutron star equation of state.

Core collapse supernova and merger of neutron stars are thought to be the origin of, respectively, long and short Gamma Ray Bursts (GRB). In both cases, a black hole will be formed and surrounded by a disk of matter. The accretion of matter onto the black hole leads to the formation of relativistic jets and the emission of gamma rays. What is interesting in this situation is that a GW signal and a GRB signal are emitted within a short delay. This may considerably enhance the detection capability, as explained below, and give deeper insight into the GRB mechanism.

Soft Gamma Repeaters (SGR) sporadically emit brief and intense bursts of soft Gamma Rays and could also be a good source of GW bursts. SGRs are produced by highly magnetized neutron stars which undergo deformations (starquakes) that could excite the modes of the star and then emit gravitational waves at about the same time as the gamma emission. The expected waveform is typically a damped sinusoid (“ringdown”) but the parameters depend on the equation of state of the nuclear matter inside the star and are not accurately known. Like in the GRB case, the gamma ray emission permits a search for the GW bursts in a narrow coincidence time window.

## 2.3 Detection methods

Based on the classification of expected sources given in the previous section, there are basically two ways of searching for GW bursts: a general one making

very little or no assumption about the signal direction, waveform, time of arrival, etc., and a second where we take benefit of an external trigger (for example a GRB) for which source location in the sky and timing are known.

The main steps of the analysis are trigger generation, efficiency estimation and accidental background estimation, whose principles are the same for both all-sky all-time unmodelled searches and triggered searches. Even with increasingly accurate predictions for GW burst waveforms, it is still mandatory that burst algorithms remain as robust as possible against the possible variety of waveform. Indeed, generic signals such as Gaussian pulses or Sine-Gaussian signals are used in parallel with astrophysical waveforms (collapse, mergers) to test the efficiency and robustness of trigger generators. The up-to-date trigger generator algorithms (or analysis “pipelines”) are time-frequency or equivalent methods looking at local excess of energy (in time and frequency) in the calibrated  $h(t)$  time series [12, 13, 14, 15, 16]. These methods can be fully coherent [12, 13, 16] taking full benefit of the existing network of detectors (LIGO and Virgo) or coincident with some coherent follow-up when looking for possible event candidates. A coherent method has the advantage that it can faithfully reconstruct the burst signal and the position of the source in the sky. Of course a coincident analysis can also reconstruct the sky location of some burst event candidate. In both cases accurate sky position can be reconstructed if the three LIGO and Virgo interferometers are in operation and in science mode at the same time. In the case of the current LIGO-Virgo network, the typical position angular accuracy is of the order a few degrees, depending on the GW direction with respect to the detectors plane [17, 18].

The efficiency estimation of the searches is performed by injecting signals in the calibrated time-shifted output data of the detectors. As already mentioned, these signals can be astrophysical signals from core-collapse or merger simulations (see for example the search for the merger and ring-down phases of binary black hole coalescences with Virgo C7 commissioning run data [19]) or generic signals. The so-called Sine-Gaussian signals (sinusoids with Gaussian envelope) are particularly interesting since they can span the detector bandwidth and give sensitivity estimates for the whole range of accessible frequencies. A number of such signals are then added to the calibrated strain of each detector after time sliding. For the all sky searches, they are generally distributed along the entire data in order to average the detectors’ noise non-stationarities. For each injected signal the amplitude described by the  $h_{\text{rss}}$ , which corresponds to the total GW signal energy:

$$h_{\text{rss}} = \sqrt{\int_{-\infty}^{+\infty} h(t)^2 dt}. \quad (1)$$

The  $h_{\text{rss}}$  amplitude has units of  $\text{Hz}^{-1/2}$ , meaning we can compare it directly to the detector sensitivities, especially when the injected waveform is well localized in frequency. The final result for each signal is the efficiency curve, detection efficiency vs.  $h_{\text{rss}}$ . Usually the  $h_{\text{rss}}$  values at 50% or 90% efficiency are chosen for setting the upper limits.

Another important aspect of the burst analysis is the background estimation and the rejection of loud outliers (glitches) using data quality flags and event by event vetoes. The quality of the detectors' data is studied at the individual detector level. Short duration noise transients can mimic a GW burst especially if their rate is large enough to induce a number of coincident events between the detectors. Data quality flags are used to indicate that one interferometer is not working properly during some period, for some known reason. Event-by-event vetoes are defined when an excess of coincidence is found between the gravitational strain channel triggers and auxiliary, environmental channel events. The above triggers are generally not obtained with the search pipelines but by other algorithms which are required to be much faster since they run on hundreds of auxiliary channels. The procedure allows us to veto only short time intervals (sub-second), thereby saving the observation time of the detectors. Once the data is cleaned by use of data quality flags and vetoes it remains to estimate the background, i.e., the number of accidental coincidences. As the noise in each detector is independent, this is done by time shifting the detector data with respect to the others and processing all these time shifted data sets with the search algorithms. Relative time shifts are chosen to be much larger than the light times of flight between the detectors and much larger than the expected signal durations.

There is a little difference for triggered searches. In this case, the data are split into an on-source region where the GW burst is expected and a background region where the noise is expected to be statistically similar to the one in the on-source region. The background region generally consists of a few hours from each side of the on-source region. All the efficiency and background studies are performed with the background data set.

All the cuts of the searches are then defined with these shifted data sets and applied in a blind way to the original unshifted data set. Events passing all the cuts (if any) are then detection candidates and can be examined more closely. If no candidate is found the result of the search can be turn into exclusion plots, for instance rate of event vs.  $h_{\text{rss}}$  in the case of all-sky analysis. The frequentist upper limit for the rate of events with confidence level  $p$  is for example [20]

$$R_p(h_{\text{rss}}) = \frac{-\ln(1-p)}{T\epsilon(h_{\text{rss}})} \quad (2)$$

where  $T$  is the observation time and  $\epsilon(h_{\text{rss}})$  is the detection efficiency for the considered waveform with amplitude  $h_{\text{rss}}$ .

## 2.4 Recent results

The search for GW bursts has not yet yielded a detection and most published results give upper limits on strain ( $h_{\text{rss}}$ ) or rate. When an astrophysical interpretation for a particular source is possible then these limits can be converted into meaningful astrophysical bounds.

The most recent all sky search for unmodelled GW bursts has been completed using data from the first calendar year of the S5 LIGO run. The analysis has been split in two parts, a search for low frequency signals in a 64-2000 Hz band [21] and a high frequency search in a 1-6kHz band [22]. The observation time  $T \simeq 270$  days sets an upper limit about 3.6 events/year for the rate of events at 90% confidence level ( $p = 0.9$  in the formula above) in the lower frequency band. In the higher frequency band the network live-time is only  $T \simeq 161$  days, resulting in an upper limit for the rates of events about 5.4 events/year at 90% confidence level. The strain limits depend on the details of the injected signals for efficiency estimates. The typical  $h_{rss}$  limit for Sine-Gaussian signals and most Gaussian pulses is below  $10^{-21} \text{ Hz}^{-1/2}$  in the low frequency band while it is up to a few  $10^{-20} \text{ Hz}^{-1/2}$  in the high frequency band. Not surprisingly the search sensitivity follows the detector sensitivities which are better at low frequencies than at high frequencies.

Another recent result concerns the search for a GW burst associated with GRB 070201 [23], detected by gamma-ray satellites. Those satellites found that the error box for the position of the GRB is centered at about 1 degree from the center of M31 (Andromeda) and overlaps the spiral arms of the galaxy. Andromeda is the closest spiral galaxy (at about 760 kpc) and an event possibly occurring at such a short distance would be outstanding. The GRB was a short one and likely progenitors for short GRBs are binary neutron star or neutron star-black hole coalescences or flares from SGR. The analysis for coalescence waveforms is presented in the next section. An unmodelled search for a GW burst in association with the GRB, yielded an upper limit for the radiated GW energy of about  $4.4 \times 10^{-4} M_{\odot} c^2$  for GW bursts lasting less than 100 ms for isotropic emission occurring at the LIGO peak sensitivity near 150Hz. This does not rule out the possibility of a SGR giant flare in Andromeda galaxy. Other searches for GW bursts associated to GRB have previously been published by the LIGO collaboration [24] and Virgo collaboration [25].

Two searches for GW bursts possibly associated with SGRs have been recently published [26,27]. The first one targeted the SGR 1806-20 and the SGR 1900+14, including a giant flare episode of SGR 1806-20 which occurred in December 2004 (during the LIGO ‘‘Astrowatch’’ period prior to the S4 run) and a storm episode of SGR 1900+14 which occurred in March 2006 (during the LIGO S5 run). Using a set of different waveforms the search was able to set upper limits at 90% confidence level on the isotropic GW emitted energies in the range  $3 \times 10^{45}$  to  $9 \times 10^{52}$  ergs for a source located at 10 kpc. These upper limits depend on the detector sensitivities and antenna patterns at the time of the Gamma emission, on the loudest event in the on-source region and the injected waveforms for efficiency estimation. It is worth noting that some theoretical models predict maximal GW emission energy as high as  $10^{49}$  ergs. This is well in the range of the SGR analysis sensitivity. The second paper is a re-analysis of the SGR 1900+14 storm of March 2006 with a different (‘‘stacking’’) method [27]. The gain in sensitivity is about one order of magnitude with respect to the first analysis [26].

A more exotic analysis is the search for GW bursts emitted by cosmic string cusps. The first reported results used the 2005 LIGO data (S4 run) [28]. The search used matched filtering as the predicted signals have simple and well parametrized waveforms. Upper-limits have been set for the rate of events and for cosmic string parameters such as string tension loop size or reconnection probability. These limits are not competitive with the ones obtained by other cosmological observations like indirect bounds from Big Bang Nucleosynthesis, but analysis of the S5 data (much longer data taking and with sensitivity twice as good) might surpass current limits in a some portion of the cosmic string parameter space.

### 3 Compact Binary Coalescence

#### 3.1 The Binary Coalescence Waveform

Coalescing binaries comprised of black holes and/or neutron stars are ideal sources for gravitational wave detectors. During the latter stages of its evolution, a binary emits gravitational radiation as the two component stars slowly spiral inwards before finally merging to form a single object which settles down to equilibrium. Indeed, the emission of gravitational waves from binary inspiral has been indirectly detected through observations of binary pulsars [29], although the current gravitational wave frequency is too low to be observed in terrestrial gravitational wave detectors. As the inspiral progresses, however, the frequency and amplitude of the gravitational waves increase. During the final seconds or minutes of inspiral and merger, the gravitational radiation emitted by systems with a mass between one and several hundred solar masses will lie in the sensitive band of ground based gravitational wave detectors.

The precise form of the binary coalescence gravitational waveform depends sensitively upon the parameters of the binary, most notably the masses and spins of the binary components. The eccentricity of the orbit will affect the emitted waveform but, in most cases, it is expected that the binary will have circularized before entering the sensitive band of ground based detectors [30, 31]. Historically, the binary coalescence has been split into three parts: a slow inspiral, a highly relativistic merger and ringdown to a final equilibrium state. Different techniques are used to calculate the waveform in each of these regimes. Depending upon the mass of the system, different stages of the evolution will emit gravitational waves at the sensitive frequency of the detector.

When the components of the binary are widely separated, the orbit decays slowly due to energy emitted in gravitational radiation, and the waveform sweeps slowly upwards in both frequency and amplitude. During this inspiral phase, theoretical waveforms calculated within the post-Newtonian framework [32] are expected to provide an accurate representation of the gravitational waveform. The post-Newtonian waveforms derived to date are sufficient for binaries comprised of neutron stars or low mass black holes (up to about



$10M_{\odot}$ ), as the merger will occur above the most sensitive frequency band of the detector.

It is expected that the end product of a binary system with total mass above  $2.0M_{\odot}$  will be a single, perturbed black hole which rings down, by emission of gravitational radiation, to an equilibrium configuration. Since stationary black holes are fully characterized by their mass and angular momentum, the excitations of higher multipoles, and in particular the quadrupole, will be radiated gravitationally [33]. The frequency and damping time for each of the ringdown modes depends upon the mass and angular momentum of the black hole and can be calculated analytically within the framework of black hole perturbation theory [34,35]. Ringdown waveforms will lie in the sensitive band of the detector for black holes with mass greater than around  $100M_{\odot}$ .

The dynamical merger of two black holes can only be modelled using full general relativistic calculations. Recent breakthroughs in numerical relativity have, for the first time, enabled the calculation of the gravitational waveform emitted during merger [10,9]. Currently, several groups are capable of numerically evolving two black holes through their final orbits, merger and ringdown [10,36,37]. The waveform for binaries whose components have comparable mass, and are non-spinning, is well characterized [38,39,40]. There have also been successes modelling the merger of neutron star binaries and neutron star black hole binaries [11,41,42,43]. Numerical investigations of the full parameter space of compact binary coalescence waveforms are ongoing.

### 3.2 Search Methods

As described above, the gravitational waveform for coalescing binaries is well modelled analytically and numerically. Signal processing theory [44] advocates the use of matched filtering to extract known signals from Gaussian noise. Matched filtering provides the backbone of searches for coalescing binaries [45, 46]. However, two substantial challenges remain: searching over the large parameter space of coalescing binary signals, and dealing with non-stationarities in the data.

The full binary coalescence waveform depends upon as many as seventeen parameters and it remains a challenge to search efficiently over the full parameter space. While some parameters, such as the amplitude and coalescence phase of the waveform, can be extracted using analytical techniques, others can only be searched by repeatedly evaluating the matched filter at numerous points across the parameter space. This is facilitated by creating a bank of template waveforms, subject to the condition that for any candidate signal only a small fraction of the signal (typically 3%) is lost due to filtering with a mis-matched waveform [47,48,49]. This method works well for binaries with non-spinning components. However, the parameter space of spinning binaries is considerably larger. Several methods of attacking this problem have been proposed, including phenomenological waveforms [50,51], restrictions to binaries with a single spin [52] and Markov Chain Monte Carlo [53,54] tech-

niques. However, the increase in both computational cost and the background rate associated with covering the spin parameter space has, to date, rendered this unfeasible. Indeed, it was been shown that searching for spinning binaries with non-spinning waveform templates provides comparable sensitivity to the currently available spinning searches — the benefits of using the improved, spinning template model are negated by the increase in false alarms, particularly in real data [55]. Investigations of the use of spinning templates in gravitational wave searches continue.

The data from gravitational wave interferometric detectors contains a significant number of non-stationary transients caused by various environmental and instrumental sources. These reduce the sensitivity of a matched filter search as loud noise transients will produce a large signal to noise ratio, even if they do not match well the gravitational wave binary coalescence signal. Many techniques have been developed to has mitigate the effect of these noise transients in the data. Among the most powerful are: data quality and veto tests which flag times of poor data quality or use auxiliary channels with known couplings to the gravitational wave channel to remove times of poor data [59], as described in Section 2.3; coincidence tests which require that a signal be observed, with consistent parameters, at widely separated sites [56]; signal consistency tests which compare the observed signal in the detector to the predicted waveform [57,58]; the use of improved ranking statistics which better separate the foreground and background by taking into account additional information, over and above the signal to noise ratio of the candidate [60]. By making use of these additional tests, searches for binary coalescences are approaching the theoretically predicted sensitivity in Gaussian noise.

### 3.3 Search Results and Future Prospects

Gravitational wave data from the GEO, LIGO, TAMA and Virgo interferometric detectors have been analyzed for coalescing binary signals. To date, no gravitational wave signal has been observed. Consequently an ever improving set of upper limits has been placed on the rate of binary coalescence as a function of the mass of the binary. Upper limits have been derived for systems ranging from neutron star binaries through to intermediate mass black hole binaries. Here, we recap the latest results and compare them with astrophysical predictions.

Astrophysical estimates of binary neutron star coalescence rates can be derived from observations of binary pulsars in the galaxy. These rates are extrapolated to the local universe under the assumption that the rate of binary coalescence follows the star formation rate in spiral galaxies, which is obtained from measurements of the blue light luminosity of galaxies [61]. Thus, results are quoted per  $L_{10}$  per year, where  $1L_{10} = 10^{10}$  times the solar blue luminosity and, for reference, the Milky Way is approximately  $1.7L_{10}$ . The predicted rate for binary neutron star coalescence is  $5 \times 10^{-5} L_{10}^{-1} \text{yr}^{-1}$ , although the rate could plausibly be as much as an order of magnitude larger [62]. To date,

there are no direct observations of black hole-neutron star or black hole-black hole binaries. Thus, rate estimates are based upon population synthesis, and yield realistic rates of  $2 \times 10^{-6} \text{ yr}^{-1} L_{10}^{-1}$  for neutron star-black hole binaries [63] and  $4 \times 10^{-7} \text{ yr}^{-1} L_{10}^{-1}$  for binary black holes [64]. In both cases, the rate could feasibly be as high as  $6 \times 10^{-5} \text{ yr}^{-1} L_{10}^{-1}$ .

The first eighteen months of the LIGO S5 data have been analyzed for gravitational wave signals from coalescing binaries with a total mass less than  $35M_{\odot}$  [65,66]. Upper limits obtained by combining the result of this analysis with results from S3 and S4 provide the most stringent bounds on the coalescence rate from gravitational wave observations. The binary neutron star coalescence rate is restricted, at 90% confidence, to be less than  $1.4 \times 10^{-2} L_{10}^{-1} \text{ yr}^{-1}$  [66]. This is a factor of thirty above optimistic rates, and several hundred above the best estimate of the rate. It is, however, interesting to note that the upper limit has improved by four orders of magnitude from the one obtained with LIGO's first science run [67]. For binary black holes, with component masses  $5 \pm 1M_{\odot}$ , the 90% rate limit is  $9 \times 10^{-4} L_{10}^{-1} \text{ yr}^{-1}$ , and for black hole-neutron star binaries, the limit is  $4 \times 10^{-3} L_{10}^{-1} \text{ yr}^{-1}$  [66]. These limits are again between one and two orders of magnitude from the upper end of astrophysical predictions, and three orders of magnitude from best estimates.

The most recent upper limits for binaries with a total mass greater than  $35M_{\odot}$  were obtained using data from the fourth LIGO science run. For binaries of total mass between  $30$  and  $80M_{\odot}$  a search with a phenomenological template family [68] of binary black hole waveforms gave an upper limit of  $\sim 1 L_{10}^{-1} \text{ yr}^{-1}$  [60]. For higher masses, a search for the ringdown portion of the signal yielded a rate limit for binary coalescences in the mass range  $100$  to  $400M_{\odot}$  of  $1.6 \times 10^{-3} L_{10}^{-1} \text{ yr}^{-1}$ . A search of the LIGO S5 data for black hole binaries with a total mass up to  $100M_{\odot}$  is being pursued [69]. This search will, for the first time, make use of full inspiral-merger-ringdown coalescence waveforms obtained by enhancing the post-Newtonian inspiral waveforms with merger and ringdowns simulated numerically [38].

The coalescence of two neutron stars or a neutron star and a black hole is one of the preferred progenitor scenarios for short-duration GRBs [70]. By making use of the known time and sky location of observed GRBs, it is possible to perform a more sensitive search of the gravitational wave data. This has been done for GRB 070201, which was a short GRB localized in a region of the sky which overlapped the Andromeda galaxy [23]. The search yielded no evidence of gravitational waves, and allowed for the exclusion of a binary coalescence progenitor in M31 with 99% confidence.

Recently data taking with the enhanced LIGO and Virgo+ detectors began. It is hoped that these detectors will achieve a factor of two sensitivity improvement over the initial detectors, which translates to almost an order of magnitude increase in the volume of the universe that can be probed for binary coalescences. In the following years, advanced gravitational wave detectors will bring an order of magnitude increase in sensitivity over the initial configurations. At this stage, astrophysical estimates predict the observation of gravitational waves from tens of binary coalescences per year.

## 4 Continuous Waves

### 4.1 Introduction

Although neutron stars in coalescing binary systems represent a relatively well-understood population of putative gravitational wave sources, with well-defined gravitational luminosities and population statistics, the same neutron stars (and even isolated neutron stars) can in principle radiate a detectable amount of gravitational radiation well before coalescence. Radio and X-ray pulsar populations give us only a hint of the vast number ( $\sim 10^9 - 10^{10}$ ) of neutron stars that exists in the Galaxy. We currently see perhaps only one in a million neutron stars as a pulsar, but any neutron star, pulsar or not, can generate continuous quasi-sinusoidal gravitational waves through rotation.

### 4.2 Sources

Any non-axisymmetric spinning neutron star will generate gravitational radiation. Although the centrifugal deformation can be expected to make it significantly oblate ( $\sim 10^{-4}$ ), this axisymmetric deformation will not itself generate gravitational radiation. Instead one requires the shape of the neutron star to be supported against relaxation to a fluid equipotential surface by a force, possibly an elastic stress force from the crust of the star, a magnetic force distorting the crustal shape or possibly a distortion caused by accretion or gravitational radiation-driven instabilities. A neutron star with its spin axis oriented towards us, at a distance  $d$ , with such a mass quadrupole moment  $Q$  around its axis of spin will generate a circularly polarised gravitational signal, at a frequency equal to twice the rotation rate  $\nu$  of the star, with amplitude

$$h_0 = \frac{16G\pi^2}{c^4} \nu^2 \frac{Q}{d}. \quad (3)$$

If the spin axis is inclined to the line-of-sight by an angle  $\iota$ , the radiation becomes elliptically polarised and the amplitude is reduced. It is often convenient to express  $Q$  as the product of an axial moment of inertia,  $I_{zz}$ , and an effective equatorial ellipticity,

$$\epsilon = \frac{I_{xx} - I_{yy}}{I_{zz}}, \quad (4)$$

where  $I_{xx}$  and  $I_{yy}$  are the other two principal moments of inertia. There are clearly two very important questions here: i) what is the size of deformation that neutron stars *could* have, given their equation of state, crystalline structure and physical environment, and ii) what deformations do they *actually* have. The answer to the first question depends critically on both the equation of state of the neutron star (and whether it is indeed a neutron star or a quark star) and its crystalline structure [71, 72]. Recent work by Horowitz and Kadau [73] has indicated that the structure may indeed be highly crystalline,

with point defects rapidly squeezed out to give breaking stains of as much as 0.1. This would allow self-supported equatorial ellipticities of perhaps  $10^{-5}$  to  $10^{-6}$ .

This second question is harder to address. Unlike in binary neutron star systems such as PSR B1913+16, PSR J0737–3039, PSR B1534+12 and PSR J1756–2251, where the orbital evolution presents convincing evidence of the very early stages of a coalescence, we have no direct evidence of spin-gravitars (that is, neutron stars whose observed spin-down is well-modelled by gravitational braking). Certainly in the case of equatorial deformation supported by crustal strength we cannot dismiss the notion that some neutron stars have perfectly annealed equipotential surfaces, with negligible axial quadrupole moment and therefore essentially no gravitational luminosity. For example, the extremely low period derivatives of millisecond pulsars hint that these neutron stars at least show very little equatorial asymmetry. At some level all neutron stars will show deformation due to internal magnetic pressures, though this only becomes relevant for the strongest of magnetars [74]. However, the story is less clear for young and/or accreting neutron stars. For both these classes there are plausible mechanisms to supply both the energy and the deformation necessary for significant gravitational luminosity (see for example [75, 76, 77]).

For an isolated neutron star we may postulate that the gravitational luminosity should be less than the rate of loss of rotational kinetic energy for a rigid body. In turn this defines an upper limit on the strain amplitude we could expect from rigid body gravitar with a spin-down rate  $\dot{\nu}$  as

$$h_0 \leq \left( \frac{5GI_{zz}}{2c^2d^2} \frac{|\dot{\nu}|}{\nu} \right)^{1/2}. \quad (5)$$

This “spin-down upper limit” falls below the 1-year strain sensitivity of both the initial LIGO and Virgo detectors for all but a small number of known radio pulsars, making these pulsars unlikely first-detection candidates. However, only a tiny fraction of the neutron star population is seen as electromagnetic pulsars, leaving the possibility of a gravitationally luminous, but electromagnetically dim, population.

### 4.3 Search methods

There is an obvious sense in which it is easier to search for a continuous quasi-sinusoidal signal than a transient inspiral or burst signal. A long-lived signal can be re-observed (or even retrospectively observed using archived data) and confirmed as astrophysical. In addition, there are radio and X-ray pulsars that accurately trace the rotational evolution of around 100 pulsars whose gravitational signal would fall in terrestrial observing bands. However, the benefits of a continuous wave search stop there. An inevitable consequence of searching for a long-duration deterministic signal containing up to  $\sim 10^{10}$  cycles is an exquisite sensitivity to its parameter values. Most obviously, a change in frequency corresponding to just one more or one fewer cycles during the

observation would represent an entirely different search, with a template for the expected signal that, as a matched filter, was insensitive to the original signal. It also becomes apparent that if the neutron star is spinning down, the number of spin-down templates necessary to cover the possible alternatives scales as the square of the observing time. Additionally, the doppler modulation of the received signal is sensitive to the position of the source on the sky. For year-long observations this angular sensitivity is approximately the gravitational diffraction limit of an aperture the diameter of the Earth's orbit about the Sun ( $\sim 1$  arcsec at typical frequencies). If we do not have the benefit of a radio trace of the neutron star's rotational evolution and sky location we are forced to perform a search over this parameter space, and it rapidly becomes apparent that the parameter space is huge. Continuous-wave searches are by far the most computationally expensive searches that the gravitational wave community undertakes, and in its most general form the problem is (and always will be) fully limited by available computing power.

No matter what its form, any coherent search method will improve its strain signal-to-noise ratio as

$$\text{snr} \propto (S_h/T)^{-1/2}, \quad (6)$$

where  $S_h$  is the detector's (strain) power spectral density at the frequency of the signal and  $T$  is the observing time. However the overall sensitivity of a search is not solely dependent on signal-to-noise ratio. The more trials that are undertaken (i.e., templates that are searched) the greater the probability of random noise popping up to unluckily appear like a signal. The apparent signal-to-noise ratio indicative of a true signal is therefore several tens for searches that pick the strongest candidate from over a wide parameter space. One consequence of this is that any convincing signal must have a relatively high signal-to-noise ratio after only a relatively short coherent integration. This allows one to combine these short integrations incoherently (as powers, ignoring phase) without too great an impact in overall sensitivity and develop semi-coherent search methods which are computationally much cheaper [78]. The overall sensitivity does however only improve as the quarter power of the number of incoherently combined contributions.

Ground-based CW search efforts have concentrated on variants of the above, from fully coherent long-timescale searches for gravitational wave signals phase-locked to radio pulsars [79, 80, 81, 82] to searches concentrating on non-pulsing targets [83, 84] and massively computational all-sky searches using a variety of semi-coherent techniques [85, 86, 87, 88, 89].

#### 4.4 Search results

Upper limits on the strength of continuous gravitational waves from both known and unknown galactic neutron stars have been made regularly since the first LIGO/GEO science run in 2002. As sensitivities and run lengths have improved, the limits have steadily dropped. The recent 23-month LIGO S5 run

had sufficient sensitivity to show that the Crab pulsar is not a gravitar (i.e., is not spinning down solely due to the emission of gravitational radiation). In itself this is no surprise – the overall energy budget of the Crab nebula and pulsar has to account for the nebula luminosity and expansion. However, the early S5 result (covering just the first 9 months of data) was sufficiently sensitive to show that less than about 3 percent of the spin-down luminosity of the Crab pulsar is due to gravitational emission [82]. The full S5 result, with a fully coherent search for gravitational emission from 116 known pulsars, including the Crab pulsar, is expected soon. Additional work is going on to use these and other newly-developed targeted algorithms to search Virgo VSR1 data for emission from the Vela pulsar at  $\sim 22.5$  Hz [90].

The S5 run has also resulted in the most sensitive “all sky” (i.e., survey) searches to date. Two early-S5 papers have already been published on this [88, 89]. The first comprised a semi-coherent search, incoherently adding 30-minute demodulated power spectra (the “power flux method”). The second was an early result from Einstein@Home, a distributed screen saver application that currently attracts about 200 000 users worldwide and returns  $\sim 100$  Tflops to search project. This method looked for coincident detections between multiple 30-hour coherent searches. Both these all-sky searches returned strain upper limits of around  $10^{-24}$  for a wide spectral band, and these are levels with real astrophysical significance. A simple argument, originally by Blanford but developed by Knipsel and Allen [91] indicates that for our Galaxy population and distribution of neutron stars, the loudest expected CW source would have a strain at Earth at about this level (under certain assumptions). Such a source would need to be within a few hundred parsecs of Earth. In addition to targeted and all-sky searches, more specialised “directed” search methods are also being used to tackle likely sky locations including globular clusters, the low-mass X-ray binary Sco-X1, the galactic centre and supernova remnants. One such search, for gravitational emission from the X-ray point source at the centre of Cas A is nearing completion and has reported an expected sensitivity also in the range  $\sim 10^{-24}$  [92]. The Ligo and Virgo Collaborations have now developed a broad suite of algorithms and methods to tack a wide range of potential sources of continuous gravitational radiation, including all-sky searches for binary sources, and the full power of these will be applied to data from the current S6/VSR2 runs.

#### 4.5 Future prospects

As with other searches that involve population statistics, the crude extrapolation holds that a factor  $\eta$  improvement in sensitivity will increase detection numbers by a factor  $\sim \eta^3$ . Clearly the physical extent of the Galaxy places an upper limit on this, but that only becomes relevant for current all-sky searches when broadband sensitivities are a factor  $\sim 100$  times their current values. Perhaps more important is a consideration of the types of neutron star that may be detectable in the future using instruments with an improved

low frequency response. Current detectors show good sensitivity only to relatively rapidly spinning pulsars, most of which are recycled millisecond pulsars with low observed spin-down rates and, probably, low gravitational luminosity. Young, glitchy pulsars are more common at gravitational frequencies below  $\sim 100$  Hz, with some of the most interesting, rapidly braked, sources closer to 10 Hz, so the low-frequency wall is a particular challenge for future continuous wave gravitational observations.

## 5 Stochastic Background

A stochastic gravitational-wave background (SGWB) refers to a long-lived random GW signal. This is generally produced by a superposition of many unresolved sources, and can be characterized as cosmological or astrophysical according to the epoch in which the GWs are generated. Cosmological backgrounds can be assumed to be approximately isotropic, unpolarized and stationary, while astrophysical backgrounds may have additional structure depending on the nature of their sources.

### 5.1 Sources

A convenient measure of the strength of a SGWB is the energy density in the GWs, per logarithmic frequency interval, in units of the critical energy density needed to close the universe:<sup>1</sup>

$$\Omega_{\text{gw}}(f) = \frac{1}{\rho_{\text{crit}}} \frac{d\rho_{\text{gw}}}{d \ln f} \quad (7)$$

Cosmological models which produce a SGWB include amplification of quantum vacuum fluctuations during inflation [93,94,95], phase transitions [96,97], pre-big-bang models [98,99,100], and cosmic (super-)string models [101,102,103,104]. Standard inflationary models generate a background of constant  $\Omega_{\text{gw}}(f)$  over many decades of frequencies, but the amplitude of such a background is already bounded by cosmic microwave background observations to be  $\Omega_{\text{gw}}(f) < 10^{-14}$  [105]. Astrophysical GW backgrounds can be generated by unresolved superpositions of sources such as cosmic string cusps [104], supernovae [106], and neutron-star instabilities [107,108].

The most stringent indirect limit on a SGWB in the frequency range of ground-based detectors comes from a constraint on the total energy density present at the time of nucleosynthesis. This big-bang nucleosynthesis (BBN) bound limits the total energy density in gravitational waves to be

$$\int \frac{df}{f} \Omega_{\text{gw}}(f) \lesssim 1.1 \times 10^{-5} (N_\nu - 3) \quad (8)$$

---

<sup>1</sup> Note that  $\rho_{\text{crit}} = (3H_0^2 c^2)/(8\pi G)$  depends on the value of the Hubble constant; it has become conventional to use the fiducial value  $H_0 = 72$  km/s/Mpc when defining  $\Omega_{\text{gw}}(f)$ .



where the effective number  $N_\nu$  of neutrino species at BBN is constrained to by  $(N_\nu - 3) < 1.44$ . [109] Note that this limit only applies to cosmological SGWBs, i.e., gravitational waves generated before the era of nucleosynthesis.

## 5.2 Search Methods

Since the amplitude of a SGWB will be much smaller than that of instrumental noise in a typical ground-based detector, one needs to exploit the expectation that while instrumental noise will be (predominantly) uncorrelated between independent detectors, the gravitational wave signals in a pair of detectors should have an average correlation

$$\langle \tilde{h}_1(f) \tilde{h}_2(f') \rangle = \frac{1}{2} \delta(f - f') \gamma_{12}(f) S_{\text{gw}}(f) \quad (9)$$

where  $\gamma_{12}(f)$  encodes the observing geometry (location and orientation of detectors 1 and 2, and in the case of an anisotropic background, the spatial distribution of the background) and  $S_{\text{gw}}(f)$  is a one-sided power spectral density for the SGWB which is given for an isotropic background by

$$S_{\text{gw}}(f) = [(3H_0^2)/(10\pi^2)] f^{-3} \Omega_{\text{gw}}(f) . \quad (10)$$

The standard search method [110] for an isotropic background cross-correlates the data from pairs of detectors using an optimal filter

$$\tilde{Q}(f) \propto \frac{\gamma_{12}(f) \mathfrak{S}_{\text{gw}}(f)}{S_1(f) S_2(f)} \quad (11)$$

where  $S_{1,2}(f)$  are the noise power spectra for the two detectors and  $\mathfrak{S}_{\text{gw}}(f)$  is the expected shape of the SGWB spectrum. The resulting search is sensitive to a background  $S_{\text{gw}}(f) = S_R \mathfrak{S}_{\text{gw}}(f)$  of strength

$$S_R^{\text{detectable}} \sim \left( 2T \int_0^\infty df \frac{[\gamma_{12}(f) \mathfrak{S}_{\text{gw}}(f)]^2}{S_1(f) S_2(f)} \right)^{-1/2} . \quad (12)$$

Note that the sensitivity of a cross-correlation search improves like the square root of the observing time  $T$ . Also, stochastic background measurements tend to be dominated by the low end of the available frequency range, because  $\gamma_{12}(f)$  oscillates with increasing  $f$  within an envelope whose leading term is  $\propto f^{-1}$  and because Eq. 10 means that a constant- $\Omega_{\text{gw}}(f)$  background has  $\mathfrak{S}_{\text{gw}}(f) \propto f^{-3}$ .

A cross-correlation search can also be used to search for an astrophysical background with a specified spatial distribution, e.g., a SGWB coming from one point on the sky [111]. More sophisticated techniques can be used to recover the spatial distribution of a measured background [112].

### 5.3 Search Results

The most stringent direct limit on  $\Omega_{\text{gw}}(f)$  was set using data from the S5 run of LIGO Livingston and LIGO Hanford [113], which set the 95% confidence level upper limit of  $\Omega_{\text{gw}}(f) < 6.9 \times 10^{-6}$  assuming  $\Omega_{\text{gw}}(f)$  to be constant over the interval  $41.5 \text{ Hz} < f < 169.25 \text{ Hz}$ . A SGWB of the excluded strength, confined to those frequencies, would contribute  $9.7 \times 10^{-6}$  to the total value of  $\Omega$ . This limit is therefore more stringent than the BBN bound (Eq. 8) and we have entered the era where ground-based GW detectors are placing new limits on gravitational wave backgrounds of cosmological origin.

The previous limit from S4 data [114], while less stringent by about an order of magnitude, already placed new restrictions on the parameters of some cosmic string models which generate GWs both before and after the era of nucleosynthesis. Additional searches of S4 LIGO data set limits on the strength of possible point-like backgrounds [115] and (by correlating LIGO Livingston data with data from the ALLEGRO bar detector) set a higher-frequency limit of  $\Omega_{\text{gw}}(915 \text{ Hz}) < 1.02$  [116]. Correlation measurements using LIGO and Virgo data are expected to improve the high-frequency measurement [117]. Further searches for anisotropic backgrounds are also being conducted.

## 6 Discussion

The current search for GW covers multiple types of signals originating from different possible astrophysical events like core collapse of massive stars and neutron star formation, coalescing binary systems of neutron stars and black holes, non-axisymmetric spinning neutron stars and signals produced by a large collection of incoherent sources. The data acquired by the most sensible GW observatories, which are at present the LIGO and Virgo interferometers, are analysed applying different methods and strategies targeted to the identification and characterisation of the signals emitted by these possible sources. Moreover, methods able to catch signals coming from unknown sources are also currently used.

The analysis of the latest scientific data, acquired during the first part of the S5/VSR1 run, did not provide any evidence of a possible detection. Upper limits on the rate of events and/or the strain amplitude  $h$  are then derived and compared to the astrophysical predictions. These limits are already valuable scientific results which reinforce and widen our knowledge of the astrophysical events involved. For example they are now approaching the plausible astrophysical values in the case of GW originating from binary coalescing systems and have already set a bound to the percentage of the spin-down luminosity of the Crab pulsar on the energy emitted in gravitational radiation. The energy density in a stochastic GW background around 100 Hz has been constrained to a limit which is more stringent than the the big-bang nucleosynthesis bound, the strongest indirect limit at those frequencies. From the analysis of the data

in coincidence with the GRB 070201 it has been possible to exclude the hypothesis of a binary merger in M31 as the progenitor of this event.

Further results from the analysis of the full S5/VSR1 run data are expected soon. Meanwhile, the analysis of the data from the S6/VSR2 run will probably, if no GW detections are found, improve the current limits, owing to the possible improvement of sensitivity of LIGO and Virgo detectors. The sensitivity of the present and future GW detectors gives the possibility of studying astrophysical events jointly with other observatories, i.e. electromagnetic and neutrino observatories, likely bringing additional information on the physics of the sources and on their characteristics. The future searches will then open the possibility of performing a mature GW astronomy.

## Acknowledgements

The authors would like to thank their colleagues in the LIGO and Virgo Scientific Collaborations, especially Ray Frey, Ben Owen and Joe Romano for comments and suggestions. SF would like to acknowledge the support of the Royal Society. JTW is supported by NSF grant PHY-0855494 and by the College of Science of Rochester Institute of Technology.

## References

1. Abbott, B.P., et al.: Rep. Prog. Phys. **72**, 076901 (2009)
2. Acernese, F., et al.: Class. Quant. Grav. **23**, S635 (2006)
3. Takahashi, R. and the TAMA Collaboration, Class. Quant. Grav. **21**, S403 (2004)
4. Lück, H., et al.: Class. Quant. Grav. **23**, S71 (2006)
5. Ott, C.D., et al.: Phys. Rev. Lett. **96**, 201102 (2006)
6. Ott, C.D., et al.: Phys. Rev. Lett. **98**, 261101 (2007)
7. Ott, C.D., et al.: Class. Quant. Grav. **24**, 139 (2007)
8. Marek, A., Janka, H.-T., Müller, E.: Astron. Astrophys. **496**, 475 (2009)
9. Baker, J. G., Campanelli, M., Pretorius, F., Zlochower, Y.: Class. Quant. Grav. **24**, S25 (2007)
10. Pretorius, F. In M. Colpi, P. Casella, V. Gorini, U. Moschella, and A. Possenti, editors, *Physics of Relativistic Objects in Compact Binaries: from Birth to Coalescence*. Springer, Heidelberg, Germany, 2009.
11. Baiotti, L., Giacomazzo, B., Rezzolla, L.: Phys. Rev. D **78**, 084033 (2008)
12. Klimentenko, S., Mitselmakher, G.: Class. Quant. Grav. **21**, S1819 (2004)
13. Klimentenko, S., et al.: Class. Quant. Grav. **25**, S114029 (2008)
14. Chatterji, S., et al.: Class. Quant. Grav. **21**, S1809 (2004)
15. Clapson, A.-C., et al.: Class. Quant. Grav. **25**, 035002 (2008)
16. Chatterji, S., et al.: Phys. Rev. D **74**, 082005 (2006)
17. Cavalier, F., et al.: Phys. Rev. D **74**, 082004 (2006)
18. Markowitz, J., Zanolin, M., Cadonati, L., Katsavounidis, E.: Phys. Rev. D **78**, 122003 (2008)
19. Acernese, F., et al.: Class. Quant. Grav. **26**, 085009 (2009)
20. Brady, P.R., Creighton, J.D.E., and Wiseman, A.G.: Class. Quant. Grav. **21**, S1775-S1782 (2004)
21. Abbott, B.P., et al.: arXiv:0905.0020 [gr-qc].
22. Abbott, B.P., et al.: arXiv:0904.4910 [gr-qc].
23. Abbott, B.P., et al.: Astrophys. J. **681**, 1419 (2008)
24. Abbott, B.P., et al.: Phys. Rev. D **77**, 062004 (2008)

25. Acernese, F., et al.: *Class. Quant. Grav.* **25**, 225001 (2008)
26. Abbott, B.P., et al.: *Phys. Rev. Lett.* **101**, 211102 (2008)
27. Abbott, B.P., et al.: *Astrophys. J.* **701**, L68 (2009)
28. Abbott, B.P., et al.: arXiv:0904.4718v2 [astro-ph.CO].
29. Weisberg, J.M., Taylor, J.H.: *ASP Conf. Ser.* **328**, 25 (2005)
30. Cokelaer, T., Pathak, D.: *Class. Quant. Grav.* **26**, 045013 (2009)
31. Martel, K., Poisson, E.: *Phys. Rev. D* **60**, 124008 (1999)
32. Blanchet, L.: *Liv. Rev. Rel.* **9**, 3 (2006)
33. Berti, E., Cardoso, V., Will, C.M.: *Phys. Rev. D* **73**, 064030 (2006)
34. Chandrasekhar, S., Detweiler, S.: *Proc. Roy. Soc. Lon.* **A344**, 441 (1975)
35. Leaver, E.W.: *Proc. Roy. Soc. Lon.* **A402**, 285 (1985)
36. Husa, S.: *Eur. Phys. J. ST* **152**, 183 (2007)
37. Hannam, M.: *Class. Quant. Grav.* **26**, 114001 (2009)
38. Buonanno, A., et al.: *Phys. Rev. D* **76**, 104049 (2007)
39. Damour, T., Nagar, A.: *Phys. Rev. D* **77**, 024043 (2008)
40. Ajith, P., et al.: *Class. Quant. Grav.* **24**, S689 (2007)
41. Duez, M.D., et al.: *Phys. Rev. D* **78**, 104015 (2008)
42. Read, J.S., et al.: *Phys. Rev. D* **79**, 124033 (2009)
43. Shibata, M., Taniguchi, K.: *Phys. Rev. D* **77**, 084015 (2008)
44. Wainstein, L.A., Zubakov, V.D.: Prentice-Hall, Englewood Cliffs, NJ, 1962.
45. Finn, L.S., Chernoff, D.F.: *Phys. Rev. D* **47**, 2198 (2219)1993
46. Allen, B.A., Anderson, W.G., Brady, P.R., Brown, D.A., Creighton, J.D.E.: arXiv:gr-qc/0509116.
47. Owen, B.J.: *Phys. Rev. D* **53**, 6749–6761 (1996)
48. Owen, B.J., Sathyaprakash, B.S.: *Phys. Rev. D* **60**, 022002 (1999)
49. Babak, S., et al.: *Class. Quant. Grav.* **23**, 5477 (2006).
50. Buonanno, A., Chen, Y., and Vallisneri, M.: *Phys. Rev. D* **67**, 104025 (2003) Erratum *Phys. Rev. D* **74**, 029904(E) (2006)
51. Abbott, B., et al.: *Phys. Rev. D* **78**, 042002 (2008)
52. Pan, Y., Buonanno, A., Chen, Y., Vallisneri, M.: *Phys. Rev. D* **69**, 104017 (2004) Erratum *Phys. Rev. D* **74**, 2006 (029905(E))
53. van der Sluys, M.V., et al.: *Astrophys. J. Lett.* **688**, L61 (2008)
54. van der Sluys, M. et al.: *Class. Quant. Grav.* **25**, 184011 (2008)
55. Van Den Broeck, C., et al.: *Phys. Rev. D* **80**, 024009 (2009)
56. Robinson, C.A.K., Sathyaprakash, B.S., Sengupta, A.S.: *Phys. Rev. D* **78**, 062002 (2008)
57. Allen, B.: *Phys. Rev. D* **71**, 062001 (2005)
58. Rodríguez, A.: Master's thesis, Louisiana State University, 2007
59. Christensen, N., Shawhan, P., González, G.: *Class. Quant. Grav.* **21**, S1747 (2004)
60. Abbott, B., et al. *Phys. Rev. D* **77**, 062002 (2008)
61. Kopparapu, R.K., et al.: arXiv:0706.1283 [astro-ph].
62. Kalogera, V., et. al: *Astrophys. J. Lett.* **601**, L179 (2004) Erratum *Astrophys. J. Lett.* **614**, 2004 (L137)
63. O'Shaughnessy, R., Kim, C., Kalogera, V., Belczynski, K.: *Astrophys. J.* **672**, 479 (2008)
64. O'Shaughnessy, R., et al.: *Astrophys. J.* **633**, 1076 (2005)
65. Abbott, B.P., et al.: *Phys. Rev. D* **79**, 122001 (2009)
66. Abbott, B., et al.: arXiv:0905.3710 [gr-qc].
67. Abbott, B., et al.: *Phys. Rev. D* **69**, 122001 (2004)
68. Buonanno, A., Chen, Y., Vallisneri, M.: *Phys. Rev. D* **67**, 024016 (2003)
69. Robinson, C., for the LIGO Scientific Collaboration and Virgo Collaboration: ligo-g0900596-v2 (2009)  
<http://dcc.ligo.org/cgi-bin/DocDB/ShowDocument?docid=G0900596>
70. Nakar, E.: *Phys. Rep.* **442**, 166 (2007)
71. Ushomirsky, G., Cutler, C., Bildsten, L.: *Mon. Not. R. Astron. Soc.* **319**, 902 (2000)
72. Owen, B.J.: *Phys. Rev. Lett.* **95**, 211101 (2005)
73. Horowitz, C.J., Kadau, K. : *Phys. Rev. Lett.* **102**, 191102 (2009)
74. Colaiuda, A., Ferrari, V., Gualtieri, L., Pons, J.A.: *Mon. Not. R. Astron. Soc.* **385**, 2080 (2008)

- 
75. Friedman, J.L., Schutz, B.F.: *Astrophys. J.* **222**, 281 (1978)
  76. Bildsten, L.: *Astrophys. J. Lett.* **501**, L89 (1998)
  77. Owen, B.J.: *Class. Quant. Grav.* **23**, S1 (2006)
  78. Cutler, C., Gholami, I., Krishnan, B.: *Phys. Rev. D* **72**, 042004 (2005)
  79. Abbott, B.P., et al.: *Phys. Rev. D* **69**, 082004 (2004)
  80. Abbott, B.P., et al.: *Phys. Rev. Lett.* **94**, 181103 (2005)
  81. Abbott, B.P., et al.: *Phys. Rev. D* **76**, 042001 (2007)
  82. Abbott, B.P., et al.: *Astrophys. J. Lett.* **683**, L45 (2008)
  83. Abbott, B.P., et al.: *Phys. Rev. D* **76**, 082001 (2007)
  84. Abbott, B.P., et al.: *Phys. Rev. D* **76**, 082003 (2007)
  85. Abbott, B.P., et al.: *Phys. Rev. D* **72**, 102004 (2005)
  86. Abbott, B.P., et al.: *Phys. Rev. D* **77**, 022001 (2008)
  87. Abbott, B.P., et al.: *Phys. Rev. D* **79**, 022001 (2009)
  88. Abbott, B.P., et al.: *Phys. Rev. Lett.* **102**, 111102 (2009)
  89. Abbott, B.P., et al.: *Phys. Rev. D* **80**, 042003 (2009)
  90. Frasca, S., for the LIGO Scientific Collaboration and Virgo Collaboration: ligo-g0900712-v1 (2009)  
<http://dcc.ligo.org/cgi-bin/DocDB/ShowDocument?docid=G0900712>
  91. Knispel, B., Allen, B., *Phys. Rev. D* **78**, 044031 (2008)
  92. Wette, K., et al.: *Class. Quant. Grav.* **25**, 235011 (2008)
  93. Grishchuk, L.P.: *Sov. Phys. JETP* **40**, 409 (1975)
  94. Grishchuk, L.P.: *Class. Quant. Grav.* **14**, 1445 (1997)
  95. Starobinsky, A.A.: *Pis'ma Zh. Eksp. Teor. Fiz.* **30**, 719 (1979)
  96. Kosowsky, A., Turner, M.S., Watkins, R.: *Phys. Rev. Lett.* **69**, 2026 (1992)
  97. Apreda, R., Maggiore, M., Nicolis, A., Riotto, A.: *Nucl. Phys. B* **631**, 342 (2002)
  98. Gasperini, M., Veneziano, G.: *Astropart. Phys.* **1**, 317 (1993)
  99. Gasperini, M., Veneziano, G.: *Phys. Rep.* **373**, 1 (2003)
  100. Buonanno, A., Maggiore, M., Ungarelli, C.: *Phys. Rev. D* **55**, 3330 (1997)
  101. Caldwell, R.R., Allen, B.: *Phys. Rev. D* **45**, 3447 (1992)
  102. Damour, T., Vilenkin, A.: *Phys. Rev. Lett.* **85**, 3761 (2000)
  103. Damour, T., Vilenkin, A.: *Phys. Rev. D* **71**, 063510 (2005)
  104. Siemens, X., Mandic, V., Creighton, J.: *Phys. Rev. Lett.* **98**, 111101 (2007)
  105. Smith, T.L., et al.: *Phys. Rev. D* **73**, 123503 (2006)
  106. Coward, D.M., Burman, R.R., Blair, D.G.: *Mon. Not. R. Astron. Soc.* **329**, 411 (2002)
  107. Regimbau, T., de Freitas Pacheco, J.A.: *Astron. Astrophys.* **376**, 381 (2001)
  108. Regimbau, T., de Freitas Pacheco, J.A.: *Astron. Astrophys.* **447**, 1 (2006)
  109. Cyburt, R.H., et al. *Astropart. Phys.* **23**, 313 (2005)
  110. Allen, B. and Romano, J., *Phys. Rev. D* **59**, 102001 (1999)
  111. Ballmer, S., *Class. Quant. Grav.* **23**, S179 (2006)
  112. Mitra, S., et al.: *Phys. Rev. D* **77**, 042002 (2008)
  113. Abbott, B.P., et al.: *Nature* **460**, ???-??? (2009)
  114. Abbott, B., et al.: *Astrophys. J.* **659**, 918 (2007)
  115. Abbott, B., et al.: *Phys. Rev. D* **76**, 082003 (2007)
  116. Abbott, B., et al.: *Phys. Rev. D* **76**, 022001 (2007)
  117. Cella, G. et al.: *Class. Quant. Grav.* **24**, S639 (2007)